

EurJIC

European Journal of Inorganic Chemistry

 **Chemistry
Europe**

European Chemical
Societies Publishing

Accepted Article

Title: [Re(h6-C6H5-benzimidazole)2]⁺ and Derivatives as Dye Mimics; Syntheses, UV Absorption Studies and DFT Calculations

Authors: Carla Gotzmann, Olivier Blacque, Thomas Fox, and Roger Alberto

This manuscript has been accepted after peer review and appears as an Accepted Article online prior to editing, proofing, and formal publication of the final Version of Record (VoR). This work is currently citable by using the Digital Object Identifier (DOI) given below. The VoR will be published online in Early View as soon as possible and may be different to this Accepted Article as a result of editing. Readers should obtain the VoR from the journal website shown below when it is published to ensure accuracy of information. The authors are responsible for the content of this Accepted Article.

To be cited as: *Eur. J. Inorg. Chem.* 10.1002/ejic.202100294

Link to VoR: <https://doi.org/10.1002/ejic.202100294>

WILEY-VCH

FULL PAPER

[Re(η^6 -C₆H₅-benzimidazole)₂]⁺ and Derivatives as Dye Mimics; Syntheses, UV Absorption Studies and DFT Calculations

Carla Gotzmann^[a], Olivier Blacque^[a], Thomas Fox^[a] and Roger Alberto^{*[a]}

[a] Dr. Carla Gotzmann, Dr. Olivier Blacque, Dr. Thomas Fox, Prof. Dr. Roger Alberto
Department of Chemistry
University of Zurich
Winterthurerstrasse 190, 8057 Zurich, Switzerland
E-mail: ariel@chem.uzh.ch

Supporting information for this article is given via a link at the end of the document

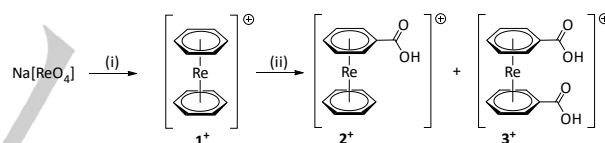
Abstract: Functionalizations of highly oxidation and hydrolysis stable mono-cationic rhenium bis-arene complexes ([Re(η^6 -C₆H₆)₂)⁺]; are of great interest. We directly built up structural features of the well-known Hoechst Dye on the coordinated arenes as a model for prospective DNA minor groove binding studies. Extensions of the aromatic bis-arene unit with functionalized and derivatized benzimidazole moieties resulted in a deep orange colour of the complexes, showing UV/Vis absorption spectra with multiple transition maxima. These have been assigned with support of DFT calculations to gain information about their charge transfer natures. The different transitions of the complexes, which are either intra-ligand, ligand-to-ligand or metal-to-ligand charge transitions, were additionally compared and discussed with the spectra of the corresponding free ligands.

Introduction

Bioorganometallic complexes have gained strong interest over the past decades. They are employed for biological and medicinal purposes but also in related fields such as environmental science, toxicology, metallomics, energy, catalysis, biosensing, radiopharmacy and as active sites in artificial and natural metalloenzymes.^[1] Metallocenes such as ferrocene, probably the most important bioorganometallic compound, pioneered the field. They are generally neutral, water- and air-stable to a certain extent and can be derivatized or functionalized in numerous ways.^{[1a],[2]} Recently, structurally and electronically related transition metal bis-arene complexes with isoelectronic, neutral and aromatic cyclic π -aromatic hydrocarbons attracted attention. Complexes comprising the [Ru(η^6 -cymene)]²⁺ substructure are core compounds in bioorganometallic cancer therapy.^[1a, 3] Sandwich complexes of the bis-arene type [M(η^6 -arene)₂]ⁿ⁺ are isoelectronic to many metallocenes and only little studied in the bioorganometallic field. Although existing for groups 6 (n=0) and 8 (n=2) in particular, they show lower kinetic and thermodynamic stabilities than their mono-arene or cyclopentadienyl analogues.^[4] Synthetically, their preparations are not routine although established e.g. along the Fischer-Hafner procedure since a long time.^[5] These bis-arene complexes are closed-shell complexes.^[6] They have been reviewed several times over the past years, underlying their importance especially in catalysis but also for the life sciences.^[4a, 7]

Amongst the bis-arene complexes of the middle transition elements, the ones of the manganese triad found probably the least attention. Rhenium and ^{99m}Tc are of central interest in

radionuclide therapy (^{186/188}Re) and imaging (^{99m}Tc). Since some time, we focus on the chemistry of highly stable, oxidation insensitive rhenium bis-arene type complexes (e.g. [Re(η^6 -C₆H₆)₂]⁺ (**1**⁺), Scheme 1).^[6c, 6d] The rationale behind is the option of coordinating either of the two elements directly to phenyl groups integrated in pharmaceuticals, without the need of a bifunctional chelator. Whereas the direct synthesis of [^{99m}Tc(η^6 -arene)₂]⁺ complexes with highly functionalized arenes was recently reported,^[8] the preparation of rhenium homologues does not work along this path. Functional modifications have to be introduced after the preparation of the basic [Re(η^6 -arene)₂]⁺ complex. Previously, we modified a procedure by Kudinov et al.^[9] and introduced basic functionalities to the coordinated arenes to yield e.g. the mono- and bis-substituted benzoic acid complexes [Re(η^6 -C₆H₅-COOH)(η^6 -C₆H₆)]⁺ (**2**⁺) and [Re(η^6 -C₆H₅-COOH)₂]⁺ (**3**⁺) (Scheme 1).^[6d]

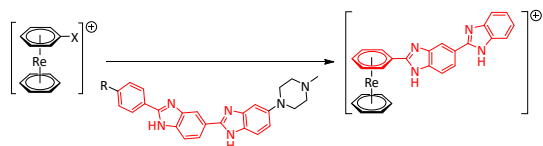


Scheme 1. Reaction pathway to obtain [Re(η^6 -C₆H₅-COOH)(η^6 -C₆H₆)]⁺ (**2**⁺) and [Re(η^6 -C₆H₅-COOH)₂]⁺ (**3**⁺) starting from Na[ReO₄].^[6d]

(i) Zn powder, AlCl₃, C₆H₆, 80°C reflux, 19h. (ii) LDA, dry THF, -78°C, 1.5 h; then CO₂-gas, -78°C, 3 h; H₂O/TFA (4:1).

Complexes **2**⁺ and **3**⁺ are excellent starting materials for further derivatizations, e.g. the coupling of biologically active molecules via peptide bond formation. Pursuing this strategy for derivatizations of **1**⁺ with bio-relevant moieties, the backbone of the prominent DNA minor groove binder Hoechst Dyes was chosen as a target.^[10] In general, a Hoechst Dye molecule consists of a head-to-tail bound bis-benzimidazole moiety, which additionally contains a methylpiperazine unit on the tail end and a functionalized phenyl ring on the head end.^{[11],[12]} In a first step, the relevant DNA-binding parts of the Hoechst Dyes were included to obtain a rhenium bis-arene complex bearing a minor groove binding moiety for potential DNA-complex binding (Scheme 2).

FULL PAPER



Scheme 2. Introduction of the DNA Binding part of the Hoechst Dye (red) to the rhenium bis-arene complex.

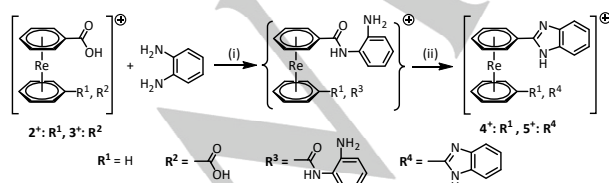
Only few studies of metal-bound Hoechst dyes are reported in literature. In both cases, a metal-containing part such as a metalloporphyrin^[13] (M = Ni, Mn) or a ruthenium phosphorescent complex^[14] was coupled to a Hoechst Dye molecule via a linker and DNA binding studies have been carried out.

To the best of our knowledge, no direct rhenium-bound Hoechst dye has been reported. DNA binding studies with a rhenium-bound Hoechst dye would allow assessing the binding mode of the complex to the DNA minor groove. From the cationic charge of the bis-arene complex, one might expect a higher binding constant than with neutral ones.

In this report, we present derivatizations with one and two benzimidazole units on **2⁺** and **3⁺** respectively, to aim a metal containing DNA minor-groove binding complexes, including adapted synthetic routes for all intermediates, full characterization and crystal structures. Furthermore, UV/Vis studies as well as corresponding time-dependent DFT calculations have been carried out to gain deeper insights into the photophysics of these colorful aromatic transition metal complexes.

Results and Discussion

Complex Syntheses. Simple amide bond formations of **2⁺** and **3⁺** with benzyl amine have been reported by our group^[6d]. The benzimidazole moieties (Bzl) on one or both of the coordinated benzene rings were obtained by reacting **2⁺** and/or **3⁺** with *ortho*-phenylenediamine via prevalent amide bond formation with activation agents such as HOBt, EDCI and DIPEA in DMF. A semi-stable mono-amide intermediate was obtained, which was isolated by preparative high-performance liquid chromatography (prep. HPLC). This intermediate "decomposed" quickly in acidic solvent media back to the starting complexes **2⁺** and **3⁺** respectively. If the reaction mixture was directly quenched with aqueous trifluoroacetic acid (TFA, 4:1, pH=1) and heated to 60–80°C overnight, an intramolecular condensation reaction (Phillips-Condensation^[15]) took place which resulted in the Bzl derivatised rhenium complexes [Re(η^6 -C₆H₅-Bzl)(η^6 -C₆H₆)]⁺ (**4⁺**) and [Re(η^6 -C₆H₅-Bzl)₂]⁺ (**5⁺**) (Scheme 3).



Scheme 3. Reaction pathways from [Re(η^6 -C₆H₆)₂]⁺ (**1⁺**) to the benzimidazole derivatised analogues [Re(η^6 -C₆H₅-Bzl)(η^6 -C₆H₆)]⁺ (**4⁺**) and [Re(η^6 -C₆H₅-Bzl)₂]⁺ (**5⁺**). (Bzl = benzimidazole)^a

(i) HOBt, EDCI, DIPEA, DMF, r.t., 16 h. (ii) H₂O/TFA (4:1), 60°C, 16h.

Complexes **[4](OTf)** and **[5](OTf)** were obtained as orange solids in moderate yields (38% and 24%) after prep. HPLC separation. The compounds with triflate (OTf) counter-ions are very well soluble in water, methanol and ethanol whereas complexes with PF₆⁻ are well soluble in non-protic solvents (dichloromethane, ethyl acetate). NMR spectra and HR-ESI-MS(+) confirmed the nature of the complexes (see supporting information). Orange single crystals for X-ray diffraction analysis could be obtained by slow evaporation of a methanol solution of **[4](PF₆)** or of **[5](OTf)**. An ORTEP is shown in Figure 1. The Re-C bond lengths to the arene ligands of **4⁺** are within a normal range of 2.230(2)–2.2606(19) Å and are comparable to other rhenium bis-arene type crystal structures.^[6c, 6d] In these and other X-ray structure analyses, the compounds show in the crystal packing extensive intermolecular π - π -stacking interactions, in general between the benzimidazole moieties and one of the coordinated arenes. Such a behavior implies the possibility of a π -stacking into DNA as expected for a Hoechst-dye like compound.

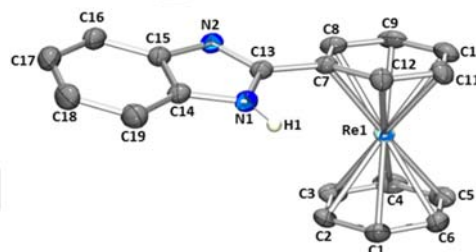
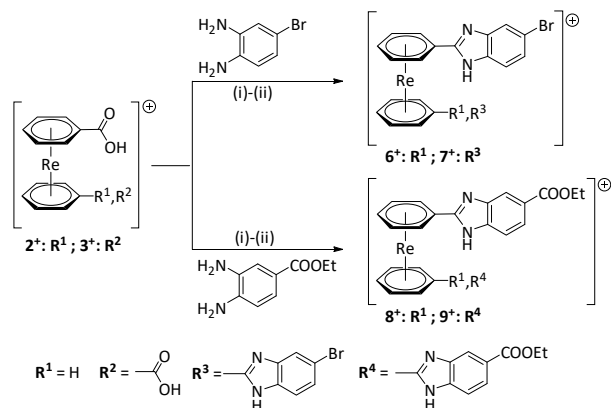


Figure 1. Ellipsoid displacement representation of [Re(η^6 -C₆H₅-Bzl)(η^6 -C₆H₆)]⁺ cation in the **[4](PF₆)** structure. Hydrogen atoms, H₂O and counter-ion are omitted for clarity; displacement ellipsoids are represented at the 50% probability level. Selected bond lengths [Å]: Re1-C1 2.249(2), Re1-C2 2.253(2), Re1-C3 2.243(2), Re1-C4 2.232(2), Re1-C5 2.234(2), Re1-C6 2.244(2), Re1-C7 2.2606(19), Re1-C8 2.243(2), Re1-C9 2.234(2), Re1-C10 2.238(2), Re1-C11 2.230(2), Re1-C12 2.238(2), C7-C13 1.471(3), C13-N1 1.346(3), C13-N2 1.336(3).

For further extending the once coupled benzimidazole system, towards a Hoechst-like system, differently functionalized 1,2-phenylenediamines were reacted with **2⁺** and **3⁺** to obtain the bromide- and ester-functionalized complex cations **6⁺** to **9⁺** (Scheme 4). The reaction procedures are similar to the one described for **4⁺** and **5⁺** including amide bond formation in a first step, followed by an internal condensation reaction. These steps led clearly to the bromo- and ester functionalized benzimidazole rhenium complexes **6⁺** - **9⁺**.

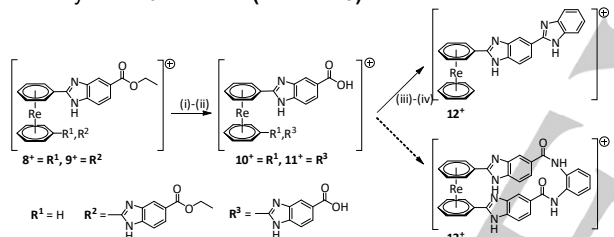
FULL PAPER

**Scheme 4.** Reaction pathways towards functionalized benzimidazole:

(i) HOBt, EDCI, DIPEA, DMF, r.t., 19–25 h. (ii) H₂O/TFA (pH=1), 50–60°C, 19–22 h.

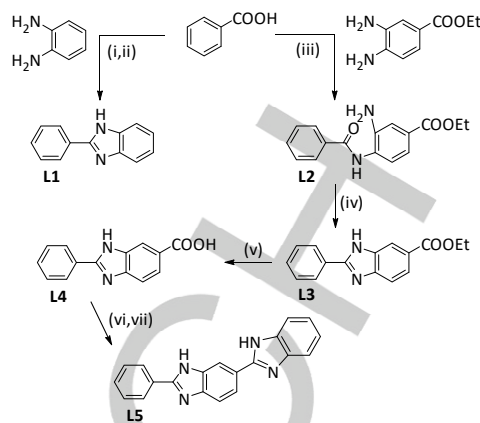
Complexes **6***–**9*** are of orange color, which are for the bis-functionalized complexes **7*** and **9*** stronger than for the mono-functionalized complexes **6*** and **8***.

Towards Hoechst dyes, the bromide substituents in **6*** and **7*** make them susceptible for nucleophilic aromatic substitution reactions. Ester-functionalized complexes **8*** and **9*** were hydrolyzed with potassium hydroxide to the corresponding carboxylates **10*** and **11*** (Scheme 5).

**Scheme 5.** Introduction of a second benzimidazole unit: (i) KOH, H₂O, r.t. 15–18 h. (ii) H₂O/TFA (pH=1). (iii) *o*-phenylenediamine, HOBt, EDCI, DIPEA, DMF, r.t., 20 h. (iv) H₂O/TFA (pH=1), 60°C, 16 h.

Reacting **10*** with another 1,2-phenylene-diamine moiety gave complex **12*** with two sequenced benzimidazole moieties. This complex is the closest mimic to the Hoechst dyes. Its authenticity was confirmed with NMR and HR-ESI-MS(+) spectroscopy (see supporting information). The synthesis of **11*** with 1,2-phenylenediamine to obtain a complex with two Bzl-Bzl moieties attached to both arene rings lead within a short reaction time to a complex with the two acid functionalities bridged by amide bonds and the formation of **13***. This compound is the kinetically favored product in the reaction as the distance of the two acid functions has been close enough to be bridged by a 1,2-diaminobenzene molecule. The color of the compound was slightly lighter orange compared to **12***, which is also confirmed in the absorption spectra. All bands are in a very similar wavelength range as found in **11*** and only differ in the epsilon values. Additionally, extensive NMR spectroscopy and HR-ESI-MS(+) confirmed the structure of **13*** (see supplementary information).

Ligand Syntheses. The pure arene-benzimidazole ligands were prepared separately for later comparison of spectroscopic data with those of the respective complexes. (Scheme 6).

**Scheme 6.** Synthetic procedure to obtain the corresponding ligands; (i) HOBt, EDCI, DIPEA, dry DMF, r.t., 3 h. (ii) H₂O/TFA (pH=1), 50°C, 15 h. (iii) HOBt, EDCI, DIPEA, DMF, r.t., 24 h. (iv) *m*-xylene/ glacial acetic acid (13:1), 80°C, 6 h. (v) KOH, MeOH, r.t. 18 h. (vi) 1,2-phenylenediamine, HOBt, EDCI, DIPEA, dry DMF, r.t., 16 h. (vii) H₂O/TFA (pH=1), 60°C, 17 h.

With the exception of **L3**, all ligands are described in the literature.^[16] Applying the synthetic route in analogy to the rhenium complexes, these ligands could be synthesized in easier and faster procedures with good yields and a more facile purification. All ligands were fully characterized to complete the analytical data and obtain corresponding spectra for the comparison with those of the rhenium complexes.

UV Absorption Studies. Electronic spectra of bis-arene rhenium complexes are scarce and UV/Vis data are only available for **1*** and a few aniline-type complexes.^[6c, 6d] The brightness of the compound colors encouraged us to investigate their electronic spectra.

All rhenium bis-arene complexes are yellow to dark orange in color while the ligands appear off-white. To obtain a deeper insight into the features of the observed electronic transitions in **1***, the mono-substituted complexes **4***, **8*** and **12*** as well as the di-substituted rhenium complexes **5*** and **9***, we analyzed the spectral maxima by TD-DFT calculations to assign the respective transitions. The participating orbitals for compounds **1***, **4***, **5***, **8***, **9***, **12*** and the corresponding neutral ligands **L1**, **L3** and **L5** are given in the supplementary information figures S81–89. Additionally the three ligands **L1**, **L3** and **L5** were investigated as well for comparison.

Figure 2 pictures the absorption spectra of **L1** (black), **L3** (red), and **L5** (blue). Three different main absorption bands are distinct. The higher energy band between 200–235 nm mainly describes $\pi \rightarrow \pi^*$ intra-ligand charge transfers (¹ILCT) amongst the benzimidazole or the phenyl ring. Ligand-to-ligand charge transfer (¹LLCT) between an occupied π -benzimidazole and an unoccupied π^* -phenyl orbital is shown in the second maximum (235–265 nm). These first two maxima are in a similar range for all three ligands, differing only in the molar extinction values ϵ . The third maximum, a ¹ILCT ($\pi_{\text{ligand}} \rightarrow \pi^*_{\text{ligand}}$) delocalized over the whole molecule, is in a range of 265–330 nm for **L1** and **L3** implicating small changes in the molecular structure. The maximum of **L5** is shifted to higher wavelengths (320–375 nm) confirming its structural difference due to the second sequenced benzimidazole moiety.

FULL PAPER

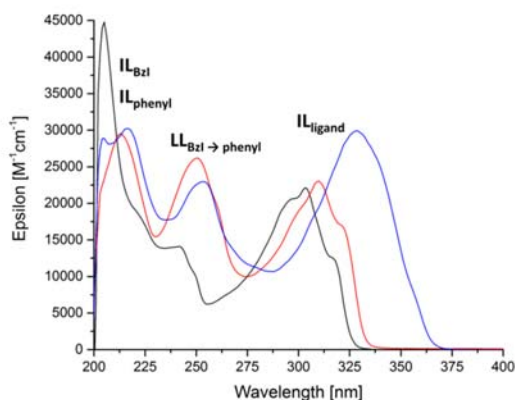


Figure 2. UV absorption spectra of the ligands L1 (black), L3 (red), L5 (blue); in methanol at room temperature.

A comparison of the absorption spectra of 1^+ and the mono-derivatised complexes 4^+ , 8^+ and 12^+ is shown in Figure 3. Beside 1^+ (black line), which displays a single band with a maximum at 265 nm indicating a metal-to-ligand charge transfer ($d_{\text{metal}} \rightarrow \pi^*_{\text{phenyl}}$) between the rhenium atom and the coordinated phenyl rings, all other complexes show at least five different transitions. The spectral characteristics of 4^+ and 8^+ are very similar and confirm that the ester moieties do not influence on the rest of the complex structures. Above 330 nm, the two maxima of 12^+ are shifted to higher wavelengths as compared to 4^+ and 8^+ .

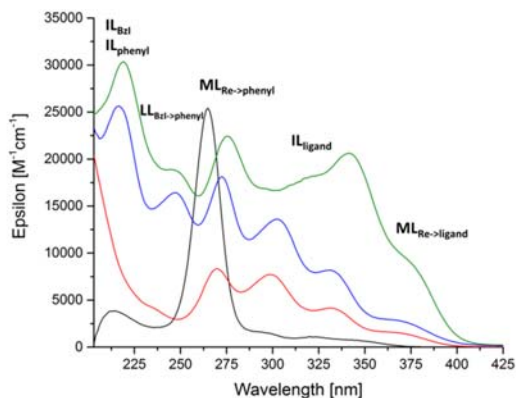


Figure 3. UV absorption spectra of 1^+ (black), 4^+ (red), 8^+ (blue) and 12^+ (green); in methanol at room temperature.

The $\pi \rightarrow \pi^*$ $^1\text{ILCT}$ transitions (210-235 nm) and $^1\text{LLCT}$ (235-260 nm) are the same as described for the corresponding ligands. In the range of 260-280 nm, all complexes show a $^1\text{MLCT}$ between occupied rhenium metal d-orbitals (HOMO) and unoccupied phenyl π^* -orbitals (LUMO). Another $^1\text{ILCT}$ transition ($\pi \rightarrow \pi^*$) is pictured between 280-360 nm, which is again of pure ligand character, delocalized over the entire molecule without any metal contribution. The lowest energy transition (360-400 nm, except 1^+) is described as another $^1\text{MLCT}$ between the HOMO (d_{metal}) and the LUMO (π^*), distributed over the whole ligand.

Figure 4 displays the absorption spectra of complex 12^+ (black) and ligand L5 (red, dashed line). This comparison verifies that three maxima are defined as $^1\text{ILCT}$ and $^1\text{LLCT}$ HOMO-LUMO transitions ($\pi \rightarrow \pi^*$) without any metal orbital influence.

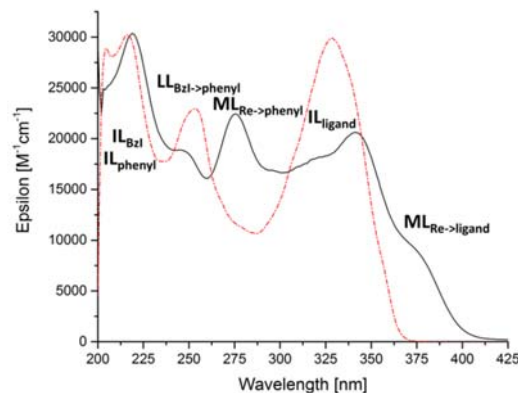


Figure 4. UV absorption spectra of 12^+ (black) and the corresponding ligand L5 (red); in methanol at room temperature.

The two remaining maxima of 12^+ are attributed to transitions involving metal orbitals. Between 270-290 nm, electron transition is executed from the d_{metal} orbitals (HOMO) into the π^* -orbitals (LUMO) of the phenyl rings. The low energy HOMO-LUMO transition occurs between d_{metal} and π^*_{ligand} orbitals.

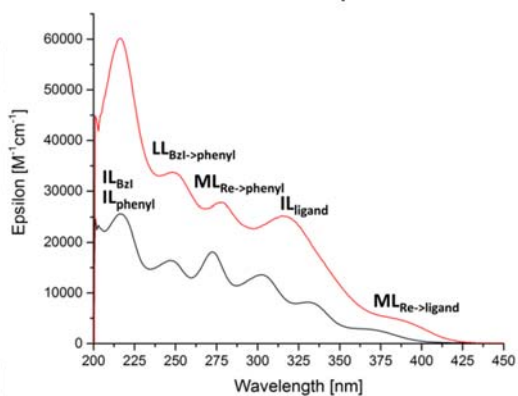


Figure 5. UV absorption spectra of 8^+ (black) and 9^+ (red), in methanol at room temperature.

Figure 5 contrasts the absorption spectra of the mono-substituted complex 8^+ with the di-substituted complex 9^+ . It is noticeable that the molar extinction values for the di-substituted complex 9^+ is roughly twice as much as the ones for 8^+ . All maxima can be found in the same wavelength range beside the intra-ligand transitions between 290-350 nm. These are more pronounced for 8^+ with two peaks, while 9^+ shows a broad maximum in this range. The lower energy $^1\text{MLCT}$ maximum is also shifted to higher wavelengths for 9^+ (around 390 nm) compared to 8^+ at around 375 nm. The complexes show weak fluorescence with emission maxima between 360 - 390 nm.

Conclusion

We showed in this study that systematic derivatisations of the basic $[\text{Re}(\eta^6\text{-C}_6\text{H}_6)_2]^+$ are feasible even with relatively complex functionalities such as the Hoechst Dye. The bio-relevant conjugated benzimidazole dyes did not affect properties such as inertness or water solubility of the rhenium scaffold. Beside synthesis and characterization, detailed UV-Vis studies have

FULL PAPER

allowed obtaining deeper insights about the photophysical properties, which could be assigned by time-dependent DFT calculations. All compounds show at least three different ILCT or LLCT transitions together with two MLCT transitions ($d_{\text{metal}} \rightarrow \pi^*_{\text{phenyl}}$ and $d_{\text{metal}} \rightarrow \pi^*_{\text{ligand}}$, respectively). These first results for metal bis-arene complexes are employed for conjugating the $[\text{Re}(\eta^6\text{-arene})_2]^+$ core to further photoactive compounds, such as photosensitizers. Corresponding biological investigations are currently performed. Preliminary DNA binding studies indicate an interaction between **12**⁺ and the DNA minor groove. These interactions are currently investigated and elaborated in more detail.

Experimental Section

General Information. Experimental methods, synthetic procedures, analytical data and NMR assignments are described in the Supporting Information for all compounds. In this section only the procedures of the key compounds **[4]**(TFA), **[5]**(TFA), **[8]**(TFA), **[10]**(OTf) and **[12]**(TFA) are given. Complexes **[1]**(OTf), **[2]**(TFA) and **[3]**(TFA) were synthesised according to literature.^[6d]

[Re($\eta^6\text{-C}_6\text{H}_5\text{-Bzl})(\eta^6\text{-C}_6\text{H}_6)](\text{TFA})$ (**[4]**(TFA)) and **[Re($\eta^6\text{-C}_6\text{H}_5\text{-Bzl})_2(\text{TFA})$** (**[5]**(TFA)). A flask was charged with **[3]**(TFA) (58.2 mg, 0.107 mmol, 1 eq.), 1,2-phenylenediamine (35.3 mg, 0.327 mmol, 3.1 eq.), HOBt (120.1 mg, 0.890 mmol, 8.3 eq.) and DMF (10 ml) under N₂. After 5 min of stirring, EDCI (164.9 mg, 0.860 mmol, 8.0 eq.) and DIPEA (220 μl , 167.2 mg, 1.289 mmol, 12.0 eq.) were added and the reaction mixture was stirred at r.t. for 16 h before evaporating the solvent. The residue was redissolved, acidified in H₂O/ TFA (10:1) and heated to 60 °C for 16 h. The solvent was removed and the crude product was purified by prep. HPLC (Gradient: prep. HPLC 1, see Supporting Information). The product containing fractions were combined and the solvent was evaporated to yield **[4]**(TFA) and **[5]**(TFA) as orange solids. Yields: 23.4 mg (0.041 mmol, 38%) for **[4]**(TFA) and 17.6 mg (0.026 mmol, 24%) for **[5]**(TFA).

Analysis of 4⁺: **¹H NMR** (500 MHz, CH₃OD): δ [ppm] = 7.62 (m, 2H, H₄), 7.33 (m, 2H, H₅), 6.96 (d, 2H, H₁), 6.37 (t, 2H, H₂), 6.21 (t, 1H, H₃), 6.04 (t, 1H, H₆). **¹³C NMR** (125 MHz, CH₃OD): δ [ppm] = 150.69 (C₆), 140.17 (C₇), 125.19 (C₅), 116.49 (C₄), 82.67 (C_a), 80.46 (C₆), 77.51 (C₃), 77.18 (C₂), 76.37 (C₁). **IR** (neat): ν [cm⁻¹]: 3078 (br), 1623 (m), 1510 (w), 1429 (s), 1362 (w), 1316 (m), 1279 (m), 1232 (w), 1151 (w), 1106 (w), 824 (s), 767 (m), 751 (s). **HR-ESI-MS** (MeOH): C₁₉H₁₆N₂Re [M]⁺; calculated, 459.08655; found, 459.08644. **UV/Vis** (MeOH): $\epsilon_{370} = 1484 \text{ M}^{-1}\text{cm}^{-1}$; $\epsilon_{331} = 4142 \text{ M}^{-1}\text{cm}^{-1}$; $\epsilon_{299} = 7720 \text{ M}^{-1}\text{cm}^{-1}$; $\epsilon_{270} = 8340 \text{ M}^{-1}\text{cm}^{-1}$; $\epsilon_{233} = 4376 \text{ M}^{-1}\text{cm}^{-1}$; $\epsilon_{203} = 20394 \text{ M}^{-1}\text{cm}^{-1}$.

Analysis of 5⁺: **¹H NMR** (500 MHz, CH₃OD): δ [ppm] = 7.11 (m, 8H, H_{4,5}), 6.91 (d, 4H, H₁), 6.46 (t, 4H, H₂), 6.24 (t, 2H, H₃). **¹³C NMR** (125 MHz, CH₃OD): δ [ppm] = 148.06 (C_b), 139.25 (C_c), 125.10 (C₅), 116.09 (C₄), 84.50 (C_a), 79.42 (C₂), 79.10 (C₃), 77.87 (C₁). **IR** (neat): ν [cm⁻¹]: 3076 (m), 2968 (w), 2138 (w), 1685 (s), 1588 (w), 1557 (w), 1495 (w), 1448 (w), 1423 (s), 1362 (w), 1314 (s), 1272 (m), 1229 (w), 1198 (m), 1183 (m), 1131 (s), 1103 (w), 1003 (m), 949 (m), 838 (s), 807 (m), 768 (s) 746 (s), 720 (m). **HR-ESI-MS** (MeOH): C₂₆H₂₀N₄Re [M]⁺; calculated, 575.12406; found, 575.12402. **UV/Vis** (MeOH): $\epsilon_{382} = 5436 \text{ M}^{-1}\text{cm}^{-1}$; $\epsilon_{310} = 19748 \text{ M}^{-1}\text{cm}^{-1}$; $\epsilon_{275} = 21340 \text{ M}^{-1}\text{cm}^{-1}$; $\epsilon_{204} = 59928 \text{ M}^{-1}\text{cm}^{-1}$.

[Re($\eta^6\text{-C}_6\text{H}_5\text{-Bzl-COOEt})(\eta^6\text{-C}_6\text{H}_6)](\text{TFA})$ (**[8]**(TFA)). A flask was charged with **[2]**(TFA) (63.3 mg, 0.127 mmol, 1 eq.), 3,4-diaminobenzoic acid ethyl ester (38.3 mg, 0.213 mmol, 1.7 eq.), HOBt (52.4 mg, 0.388 mmol, 3 eq.) and DMF (10 ml) under N₂. After 5 min of stirring, EDCI (78.1 mg, 0.407 mmol, 3.2 eq.) and DIPEA (133 μl , 101.08 mg, 0.782 mmol, 6.2 eq.) were added and the reaction mixture was stirred at r.t. for 24 h before evaporating the solvent. The orange residue was redissolved in acidified

water (with TFA, pH 1) and the reaction mixture was heated to 50 °C for 19 h. The reaction was allowed to cool to r.t., the solvent was evaporated and the crude product was purified by prep. HPLC (Gradient: prep. HPLC 2). The product containing fractions were combined and the solvent was evaporated to yield **[8]**(TFA) as an orange solid. Yield: 40.8 mg (0.064 mmol, 49%).

Analysis of 8⁺: **¹H NMR** (500 MHz, CH₃OD): δ [ppm] = 8.31 (s, 1H, H₆), 8.01 (dd, 1H, H₅), 7.67 (dd, 1H, H₄), 6.99 (d, 2H, H₁), 6.38 (t, 2H, H₂), 6.23 (t, 1H, H₃), 6.06 (s, 6H, H₉), 4.39 (q, 2H, H₇), 1.42 (t, 3H, H₈). **¹³C NMR** (125 MHz, CH₃OD): δ [ppm] = 168.28 (C_f), 153.56 (C_b), 143.05 (C_d), 140.45 (C_c), 127.26 (C_e), 126.15 (C₆), 119.04 (C₆), 115.98 (C₄), 81.77 (C_a), 80.66 (C₉), 77.43 (C₃), 77.21 (C₂), 76.47 (C₁), 62.44 (C₇), 14.80 (C₈). **IR** (neat): ν [cm⁻¹]: 3075 (m), 2981 (w), 1782 (w), 1671 (s), 1630 (w), 1512 (w), 1471 (w), 1433 (s), 1416 (w), 1394 (w), 1367 (m), 1320 (w), 1299 (s), 1197 (s), 1176 (m), 1116 (s), 1088 (w), 1023 (s), 950 (s), 888 (w), 854 (w), 831 (s), 797 (s), 768 (m), 742 (s), 717 (s), 703 (w). **HR-ESI-MS** (MeOH): C₂₂H₂₀O₂N₂Re [M]⁺; calculated, 531.10768; found, 531.10814. **UV/Vis** (MeOH): $\epsilon_{369} = 2803 \text{ M}^{-1}\text{cm}^{-1}$; $\epsilon_{331} = 8190 \text{ M}^{-1}\text{cm}^{-1}$; $\epsilon_{303} = 13607 \text{ M}^{-1}\text{cm}^{-1}$; $\epsilon_{272} = 18093 \text{ M}^{-1}\text{cm}^{-1}$; $\epsilon_{247} = 16427 \text{ M}^{-1}\text{cm}^{-1}$; $\epsilon_{216} = 25637 \text{ M}^{-1}\text{cm}^{-1}$.

[Re($\eta^6\text{-C}_6\text{H}_5\text{-Bzl-Bzl})(\eta^6\text{-C}_6\text{H}_6)](\text{TFA})$ (**[12]**(TFA)). **[10]**(OTf) (50.0 mg, 0.077 mmol, 1.0 eq.) was dissolved in DMF before 1,2-phenylenediamine (14.9 mg, 0.138 mmol, 1.8 eq.) and HOBt (33.4 mg, 0.247 mmol, 3.2 eq.) were added under N₂. After 10 min of stirring, EDCI (44.5 mg, 0.232 mmol, 3.0 eq.) and DIPEA (79 μl , 60.0 mg, 0.463 mmol, 6.0 eq.) were added and the reaction mixture was stirred at r.t. for 20 h before evaporating the solvent. The orange residue was taken up in acidified H₂O (with TFA; 20:1) and heated for 16 h at 60 °C. The reaction mixture was allowed to cool to r.t., the solvent was evaporated and the crude mixture was purified by prep. HPLC (Gradient: prep. HPLC 3). Pure product containing fractions were combined and the solvent was evaporated to afford **[12]**(TFA) as an orange solid. Yield: 10.1 mg (0.015 mmol, 19%)

Analysis of 12⁺: **¹H NMR** (500 MHz, CH₃OD): δ [ppm] = 8.47 (dd, 1H, H₇), 8.07 (dd, 1H, H₆), 7.94 (dd, 1H, H₅), 7.84 (m, 2H, H_{8/11}), 7.64 (m, 2H, H_{9/10}), 7.05 (d, 2H, H₄), 6.41 (t, 2H, H₂), 6.25 (t, 1H, H₃), 6.09 (s, 6H, H₄). **¹³C NMR** (125 MHz, CH₃OD): δ [ppm] = 155.06 (C_b), 151.69 (C_f), 143.39 (C_d), 141.89 (C_c), 133.35 (C_{g/h}), 127.91 (C_{9/10}), 124.18 (C₆), 118.98 (C_e), 117.95 (C₇), 117.75 (C₅), 114.95 (C_{8/11}), 81.39 (C_a), 80.76 (C₄), 77.47 (C₃), 77.31 (C₂), 76.61 (C₁). **IR** (neat): ν [cm⁻¹]: 3067 (br), 2655 (w), 1664 (s), 1629 (m), 1575 (m), 1519 (m), 1455 (w), 1438 (w), 1421 (w), 1410 (w), 1395 (w), 1308 (m), 1271 (w), 1233 (w), 1180 (s), 1127 (s), 1006 (m), 947 (m), 923 (w), 899 (m), 829 (s), 796 (s), 753 (s), 719 (s). **HR-ESI-MS** (H₂O): C₂₆H₂₀N₄Re [M]⁺; calculated, 575.12406; found 575.12426. **UV/Vis** (MeOH): $\epsilon_{374} = 9163 \text{ M}^{-1}\text{cm}^{-1}$; $\epsilon_{341} = 20627 \text{ M}^{-1}\text{cm}^{-1}$; $\epsilon_{321} = 18160 \text{ M}^{-1}\text{cm}^{-1}$; $\epsilon_{275} = 22430 \text{ M}^{-1}\text{cm}^{-1}$; $\epsilon_{243} = 18850 \text{ M}^{-1}\text{cm}^{-1}$; $\epsilon_{219} = 30370 \text{ M}^{-1}\text{cm}^{-1}$.

Acknowledgements

This study was financially supported by the University of Zurich.

Keywords: Sandwich Complexes, Bioorganometallic Chemistry, Hoechst Dye, Rhenium

Conflict of Interest

The authors declare no conflict of interest.

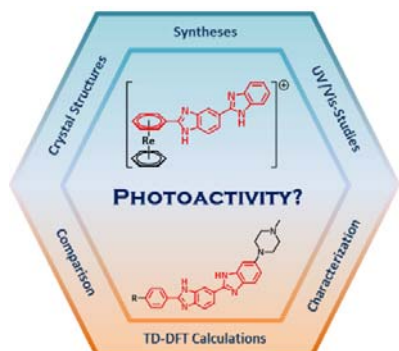
FULL PAPER

References

- [1] a) C. G. Hartinger, P. J. Dyson, *Chem. Soc. Rev.* **2009**, *38*, 391-401; b) G. Jaouen, W. Beck, M. J. McGlinchey, *Bioorganometallic Chemistry: Applications in Drug Discovery, Biocatalysis and Imaging*, Wiley-VCH, Weinheim, **2006**; c) G. Gasser, I. Ott, N. Metzler-Nolte, *J. Med. Chem.* **2011**, *54*, 3-25; d) E. A. Hillard, G. Jaouen, *Organometallics* **2011**, *30*, 20-27; e) R. Alberto, *J. Organomet. Chem.* **2007**, *692*, 1179-1186; f) M. F. R. Fouda, M. M. Abd-Elzaher, R. A. Abdelsamaia, A. A. Labib, *Appl. Organomet. Chem.* **2007**, *21*, 613-625.
- [2] M. Patra, G. Gasser, *Nature Rev. Chem.* **2017**, *1*, 0066.
- [3] P. Y. Zhang, P. J. Sadler, *J. Organomet. Chem.* **2017**, *839*, 5-14.
- [4] a) G. Pampaloni, *Coord. Chem. Rev.* **2010**, *254*, 402-419; b) R. Pettinari, A. Petrini, F. Marchetti, C. Pettinari, T. Riedel, B. Therrien, P. J. Dyson, *Eur. J. Inorg. Chem.* **2017**, 1800-1806; c) D. S. Perekalin, E. E. Karslyan, P. V. Petrovskii, A. O. Borissova, K. A. Lyssenko, A. R. Kudinov, *Eur. J. Inorg. Chem.* **2012**, 1485-1492.
- [5] E. O. Fischer, W. Hafner, *Z. Naturforsch. B* **1955**, *10*, 665-668.
- [6] a) M. Benz, H. Braband, P. Schmutz, J. Halter, R. Alberto, *Chem. Sci.* **2015**, *6*, 165-169; b) E. L. Muetterties, J. R. Bleeke, E. J. Wucherer, T. Albright, *Chem. Rev.* **1982**, *82*, 499-525; c) D. Hernández-Valdés, G. Meola, H. Braband, B. Spingler, R. Alberto, *Organometallics* **2018**, *37*, 2910-2916; d) G. Meola, H. Braband, P. Schmutz, M. Benz, B. Spingler, R. Alberto, *Inorg. Chem.* **2016**, *55*, 11131-11139.
- [7] a) G. Pampaloni, *Coord. Chem. Rev.* **2010**, *254*, 387-389; b) B. Therrien, *Coord. Chem. Rev.* **2009**, *253*, 493-519.
- [8] Q. Nadeem, G. Meola, H. Braband, R. Bolliger, O. Blacque, D. Hernandez-Valdes, R. Alberto, *Angew. Chem. Int. Ed.* **2020**, *59*, 1197-1200.
- [9] E. A. Trifonova, D. S. Perekalin, K. A. Lyssenko, A. R. Kudinov, *J. Organomet. Chem.* **2013**, *727*, 60-63.
- [10] a) M. P. Barrett, C. G. Gemmill, C. J. Suckling, *Pharmacol. Ther.* **2013**, *139*, 12-23; b) J. Portugal, M. J. Waring, *Biochim. Biophys. Acta* **1988**, *949*, 158-168; c) P. G. Baraldi, A. Bovero, F. Fruttarolo, D. Preti, M. A. Tabrizi, M. G. Pavani, R. Romagnoli, *Med. Res. Rev.* **2004**, *24*, 475-528.
- [11] K. Mišković, M. Bujak, M. B. Lončar, L. Glavaš-Obrovac, *Archives of Industrial Hygiene and Toxicology* **2013**, *64*, 593.
- [12] S. A. Latt, G. Stetten, *J. Histochem. Cytochem.* **1976**, *24*, 24-33.
- [13] S. Frau, J. Bernadou, B. Meunier, *Bioconjugate Chem.* **1997**, *8*, 222-231.
- [14] D. Hara, Y. Umehara, A. Son, W. Asahi, S. Misu, R. Kurihara, T. Kondo, K. Tanabe, *ChemBioChem* **2018**, *19*, 956-962.
- [15] M. A. Phillips, *J. Chem. Soc.* **1928**, *0*, 2393-2399.
- [16] a) D. W. Hein, R. J. Alheim, J. J. Leavitt, *J. Am. Chem. Soc.* **1957**, *79*, 427-429; b) M. A. Phillips, *J. Chem. Soc.* **1928**, 172-177; c) Y.-H. So, J. P. Heeschen, *J. Org. Chem.* **1997**, *62*, 3552-3561.

FULL PAPER

Entry for the Table of Contents



Mono- and di-substituted positive-charged Rhenium-(η^6 -arene) complexes with different functionalized and derivatized benzimidazole units have been synthesized and characterized. UV/Vis studies assisted by DFT calculations give deeper insights into the nature of the absorptions of the complexes.